



This is the submitted manuscript before review. Final published version is available as:

M. Islam and R. Martinez-Duarte, Tuning the mechanical stiffness of lightweight carbon origami, *Materials Today: Proceedings*, <https://doi.org/10.1016/j.matpr.2020.06.371>

Please cite accordingly

Tec.Nano 2019

## Tuning the mechanical stiffness of Lightweight Carbon Origami

Monsur Islam<sup>a,b</sup> and Rodrigo Martinez-Duarte<sup>a,\*</sup>

<sup>a</sup>*Multiscale Manufacturing Laboratory, Mechanical Engineering Department, Clemson University, Clemson, 29634, United States*

<sup>b</sup>*Institute of Microstructure Technology, Karlsruhe Institute of Technology, Hermann-von-Helmholtz-Platz 1, 76344 Eggenstein-Leopoldshafen, Germany*

---

### Abstract

Carbon origami has been recently reported to enable the fabrication of lightweight, 3D and architected shapes of carbon materials using renewable cellulose paper as the carbon precursor. Here, we characterize the effect of different processing variables on the mechanical stiffness of carbon origami shapes. The study is conducted using a Miura-ori pattern. The processing variables studied here include the geometrical features of the unit cell of a Miura-ori pattern, carbonization conditions, and thickness of the cellulose paper. Change of the carbonization environment exhibits a stronger impact on the density and mechanical properties of the carbon origami structure, compared to the effect of final temperature of the carbonization process. Furthermore, the elastic modulus exhibited a proportional relation to a design angle  $\alpha$  and an inversely proportional relation to a folding angle  $\beta$ . The elastic modulus of a carbon Miura-ori further increases with the thickness of the paper used for fabrication of the precursor origami shape. We compare the mechanical stiffness obtained from all the variables, which shows that a combination of  $\alpha$  and  $\beta$  exhibits the most dominant effect. Combination of all these effects can potentially lead to fabrication of a carbon origami shape that can exhibit mechanical stiffness superior to state-of-the-art cellular materials at a given low density. Further optimization of the processing parameters is needed to achieve such a carbon origami structure.

© 2019 Elsevier Ltd. All rights reserved.

---

\* Corresponding author. Tel.: +1-864-656-5634; fax: +1-864-656-4435.

E-mail address: [rodrigm@clemson.edu](mailto:rodrigm@clemson.edu)

Peer-review under responsibility of the scientific committee of the International Conference on Nanotechnology Tec.Nano 2018.

*Keywords:* Carbon; Origami; Miura-ori; Cellulose paper; Architected

---

## 1. Introduction

Carbon cellular materials are an interesting class of lightweight materials that exhibit several interesting properties including high specific strength and stiffness, excellent chemical and thermal inertness, high surface to volume ratio, and adjustable electrical conductivity [1]. Among different carbon allotropes, biopolymer derived carbon has been of interest of several researchers for fabrication of the cellular carbon materials due to abundance of the biopolymers in nature [2–6]. However, shaping of these biopolymer-derived cellular carbon materials into 3D complex geometries has not been given much attention till date. Towards fabrication of 3D complex architectures of the biopolymer-derived carbon materials, we recently reported an origami-inspired technique using cellulosic paper of plant origin as carbon precursor to obtain very low-density 3D cellular structures of high specific strength [7], as well as the implications of using other renewable films, i.e. rice paper and bacterial cellulose, in the properties of the carbon origami [6]. In such works, we shaped the cellulose paper into 3D complex shapes using origami folding and carbonized them in an inert atmosphere. Using this methodology, we were able to fabricate several 3D complex shapes of cellular carbon, which are otherwise challenging to achieve through traditional machining or pressing processes. Such origami shapes exhibited excellent load-carrying capability at a low density, which was advantageous when compared to other cellular materials such as carbon nanotube foam, graphene elastomer, metallic microlattices and silica aerogels. However, the absolute value of the stiffness of these carbon origami shapes was lower than other cellular materials. We believe that the carbon origami technique has the potential to produce structures with significantly superior mechanical stiffness than other cellular materials at a low density. However, to achieve a high stiffness carbon origami structure, it is essential to study the effect of different processing variables on its mechanical properties. Such study can further lead to customization of the carbon origami technique so that it can produce application-specific structural properties.

Here, we present the effect of different processing variables of the carbon origami technique on the mechanical stiffness of the origami structures. We focus our study on a Miura-ori pattern, due to its growing interest among the engineering communities, which has led to use of the Miura-ori patterns in different applications including space exploration and energy storage devices [8,9]. The processing variables we study here include the geometrical features of the unit cell of a Miura-ori pattern, the carbonization conditions, and thickness of the paper used to obtain the precursor origami shape. We characterize the elastic modulus of the carbon Miura-ori shapes for each of the variables by performing compression tests. We further compare the elastic moduli for all the processing variables to recognize the most influential variables that can lead to a superior mechanical stiffness.

## 2. Materials and methods

### 2.1. Precursor Materials

Fisherbrand pure cellulose chromatography (CG) paper (Sigma Aldrich, Cat. No. 05-714-1) with a thickness of 190  $\mu\text{m}$  and Whatman 3MM Chromatography paper (Sigma Aldrich, Cat. No. 3030-6158) with a thickness of 340  $\mu\text{m}$  were used for fabrication of paper origami.

### 2.2. Fabrication Procedure

The fabrication of the carbon origami shapes has been detailed in our recent publications [7,10]. Briefly, we first designed the geometries of the crease patterns in SolidWorks, a CAD software. Unit cell of a Miura-ori fold is presented in Figure 1a. The unit is defined with three design parameters:  $a$ ,  $b$  and  $\alpha$ , as indicated by the bold red font in Figure 1a. All the Miura-ori patterns designed here featured  $a = 3.1$  mm and a 3:5 ratio between  $a$  and  $b$ . We varied  $\alpha$  between  $41^\circ$  and  $75^\circ$  to investigate the effect of  $\alpha$  on the carbon Miura-ori properties. Separate crease patterns were designed for each side of the paper.

Using the designed crease patterns, the chromatography paper was pre-creased using a modified cutting plotter machine (Graphtec CE6000-40, USA), using optimized parameters. Alignment of the crease patterns on the both sides was implemented by the registration marks generated by the cutting-plotter software and printed on the paper. Upon completion of the pre-creasing step, the chromatography paper was manually folded along the crease-lines to obtain the paper origami shape. A folding angle  $\beta$  appeared in the folded origami shapes.

In the final step, the paper origami structures were carbonized in a tube furnace (TF1700, Across International, US) in an inert atmosphere to obtain carbon origami structures. Different final carbonization temperature, 900 and 1300°C, and carbonization environments, vacuum and nitrogen, were used in different combinations to investigate the effect of carbonization conditions on the properties of the carbon Miura-ori structures. Examples of carbon Miura-ori structures with different  $\alpha$  are presented in Figure 1b and c.

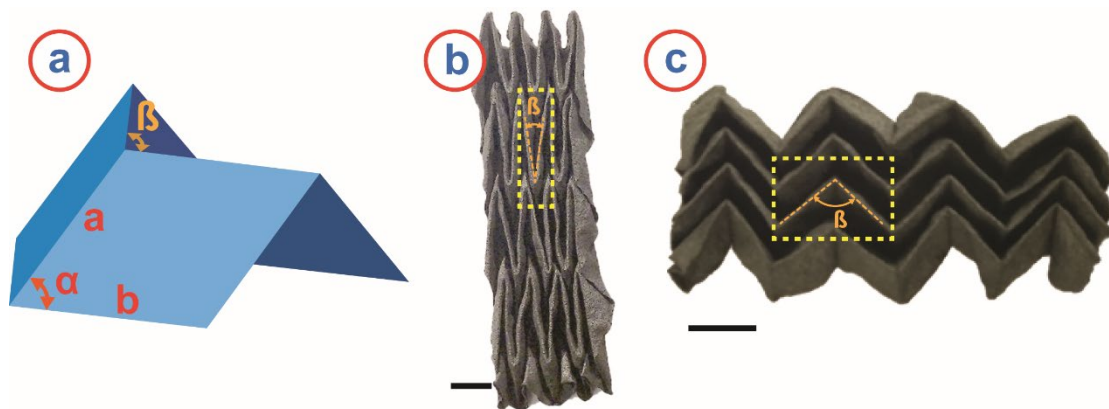


Figure 1: (a) Schematic illustration of a unit cell of a Miura-ori pattern, showing the design parameters  $a$ ,  $b$  and  $\alpha$ , and folding angle  $\beta$ . Example of carbon Miura-ori shape with (b)  $\alpha=41^\circ$  and (c)  $\alpha=75^\circ$ . A unit cell in the both Miura-ori is indicated by the yellow dashed rectangle. The folding angle  $\beta$  is also indicated in the unit cell to show how  $\beta$  changes with  $\alpha$ . Scale bar in image (b) and (c) = 5mm.

### 2.3. Structure Characterization

The morphology and microstructure of the carbon origami samples were studied using scanning electron microscopy (SEM, S4800, Hitachi, Japan). Pore sizes of the carbonized samples were measured using the SEM images using ImageJ (<https://imagej.nih.gov/ij/>), an image processing software. It should be mentioned that pores are three-dimensional features, whereas SEM images can exhibit only their 2D projections. Hence, SEM images cannot provide detailed information of the pores. However, it can provide an estimation of the pore size distribution of the carbonized samples. The structural density of the Miura-ori samples was determined using the envelope method [11–13], that is calculating the ratio of the mass of the Miura-ori structure and the overall volume occupied by it. To characterize the mechanical properties, we performed compression tests of the Miura-ori structures at a compression rate of 1 mm/min using a load cell of 50 N in an Instron Single Column Testing System (Model 5944).

## 3. Results and discussion

### 3.1. Effect of carbonization temperature and environment

The effect of carbonization conditions was studied using the Miura-ori patterns with an  $\alpha=41^\circ$ . The elastic modulus of the carbon Miura-ori structures is presented in Figure 2a. The use of a vacuum environment for carbonization had a more drastic effect on the elastic modulus when compared to the change of final temperature of the carbonization in nitrogen. For example, when the final carbonization temperature was increased from 900°C to 1300°C, the elastic modulus decreased from  $193.83\pm 32.17$  kPa to  $139.52\pm 36.89$  kPa. However, when the carbonization environment was

changed to vacuum, the elastic modulus decreased to  $45.98 \pm 13.50$  kPa. Such change in the mechanical properties can be explained by the change in the microstructure of the carbon origami structures at different carbonization conditions. In general, the carbon origami structures featured a randomly distributed microfibril network (Figure 2b) with an average fiber diameter of  $5.26 \pm 2.53$   $\mu\text{m}$ . However, when inspecting the individual carbon microfibers, different microstructures were observed at different carbonization conditions. For the final temperature of  $900^\circ\text{C}$  in the nitrogen environment, the carbon microfibers featured numerous mesopores (pore diameter 2 – 21 nm), as shown in Figure 2c. The escape of gaseous substances during thermal decomposition of the precursor cellulose might have resulted in such mesopores. Increasing temperature up to  $1300^\circ\text{C}$  in the nitrogen environment did not exhibit any drastic change in the microstructure (Figure 2d), although presence of many micropores (pore diameter  $< 2$  nm) were observed along with

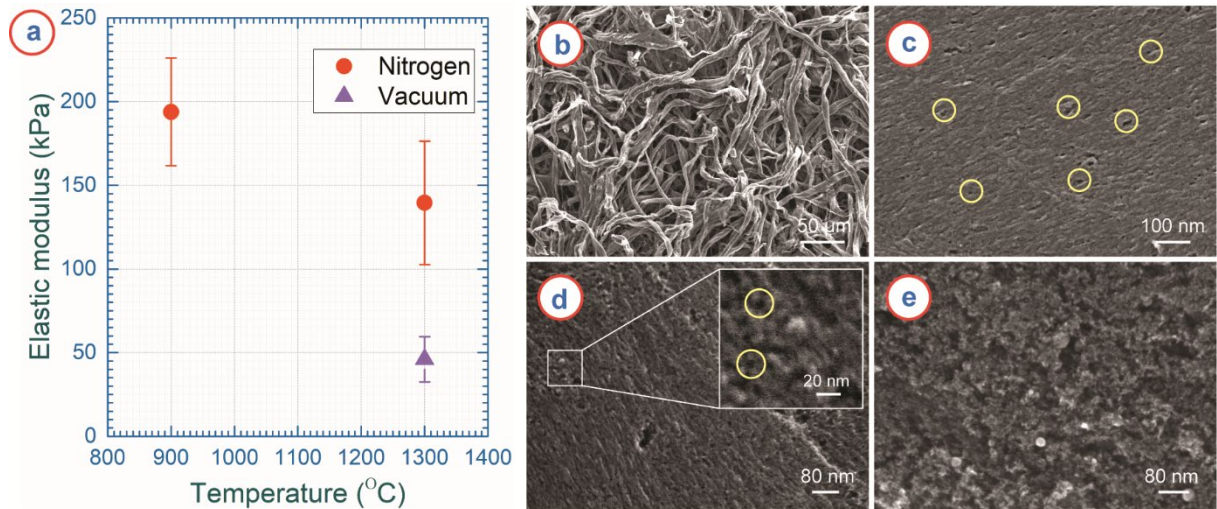


Figure 2: (a) Variation of elastic modulus of the carbon Miura-ori shapes obtained at different temperatures and using different heating environment. (b) SEM image of the carbon origami structure showing randomly distributed microfibril microstructure. High magnification SEM image of individual microfibers obtained for carbonization conditions of (c) a final temperature of  $900^\circ\text{C}$  in a nitrogen environment, (d) a final temperature of  $1300^\circ\text{C}$  in a nitrogen environment and (e) a final temperature of  $1300^\circ\text{C}$  in a vacuum environment. The circles in (c) indicate occurrences of mesopores micropores in the carbon fibers. Inset of (d) is magnified image of the section indicated by rectangle, which shows occurrences of micropores. Examples of such micropores are indicated by the circles as well.

mesopores as shown in the inset of Figure 2d. Occurrence of such micropores might occur due to further weight loss at higher temperature. Because of such high temperature weight loss, an increasing temperature resulted in a relatively lower density. As the elastic modulus of a cellular architecture relates proportionally to its structural density [14], the obtained lower density at a higher temperature yielded a relatively lower elastic modulus. However, there were overlaps of the data points for elastic modulus of the samples obtained at  $1300^\circ\text{C}$  with that of  $900^\circ\text{C}$ , as evidenced by the standard deviations in the measurements (Figure 2a). Such overlaps can be attributed to the similar microstructures of both samples. In comparison to a nitrogen environment, a vacuum environment resulted in a more porous and rougher microstructure of the carbon microfibers, as shown in Figure 2e. Such highly porous microstructure was attributed to the aggressive thermal decomposition in the vacuum environment, compared to any inert gas environment, which further results in higher weight loss during carbonization [15]. Such phenomena yielded a lower density and a lower elastic modulus of the carbon Miura-ori for vacuum carbonization, in comparison to nitrogen environment.

### 3.2. Effect of folding angle

The overall of geometry of a Miura-ori depends on the design parameter  $\alpha$  of the unit cell. A larger  $\alpha$  led to formation of a wider Miura-ori structure, resulting in a larger  $\beta$  as shown in Figure b and c. However, a larger  $\alpha$  infers a more vertical sidewall, which should yield a stiffer structure. This was confirmed in Figure 3a, which shows that the

carbon Miura-ori with an  $\alpha$  of  $75^\circ$  exhibited a higher elastic modulus compared to that of  $41^\circ$ . These carbon Miura-ori samples were obtained at  $900^\circ\text{C}$  in the nitrogen environment.

The elastic modulus of the carbon Miura-ori structures is also dependent on the folding angle  $\beta$ . Figure 3a shows that the elastic modulus increased with a decreasing  $\beta$ . For example, for the Miura ori structures with  $\alpha=75^\circ$ , the elastic modulus increased from  $121.23 \pm 33.58$  kPa for  $\beta=88.9^\circ \pm 8.0^\circ$  to  $771.99 \pm 100.50$  kPa for  $\beta=17.9^\circ \pm 1.6^\circ$ . The elastic modulus followed an empirical relation with  $\beta$  as shown in Equation 1. The elastic modulus of the Miura-ori structures with  $\alpha=41^\circ$  followed the similar trend.

$$E \propto \beta^{-1.2}$$

Equation 1

As mentioned earlier, the elastic modulus of an architected structure relates proportionally to the density of the structure. For our carbon Miura-ori structures, the structural density increased for a smaller  $\beta$ , as a smaller  $\beta$  inferred to a tighter packing of the unit cells, which can be seen in the insets of Figure 3a. Therefore, the elastic modulus of the carbon Miura-ori structures increased with reducing  $\beta$ .

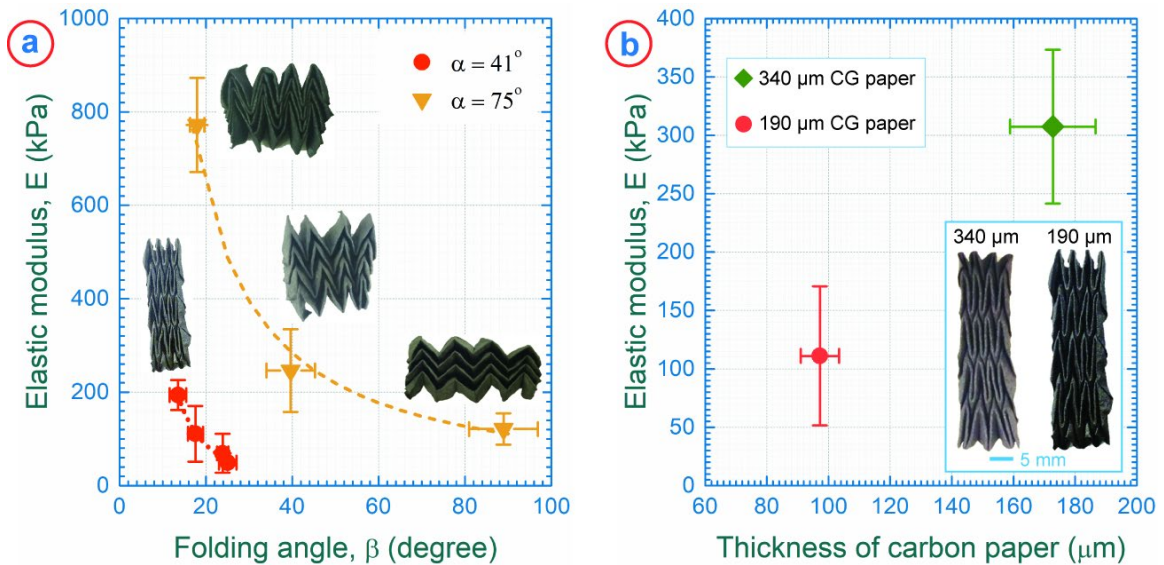


Figure 3: (a) Variation of elastic modulus of the Miura-ori structures with varying design parameter  $\alpha$  and folding angle  $\beta$ . Insets show Miura-ori patterns corresponds to different  $\beta$  and  $\alpha$ . (b) Effect of paper thickness on the elastic modulus of the carbon Miura-ori structures. Inset shows the carbon Miura-ori structures from different paper thickness, reference length bar is 5 mm for both cases.

### 3.3. Effect of paper thickness

The paper experienced around 50% shrinkage in thickness during the carbonization process. The paper thickness did not have any effect on the overall geometry of the carbon Miura-ori as shown in the inset of Figure 3b, which shows carbon Miura-ori structures derived from a 3 X 3 in CG paper with thicknesses of 190  $\mu\text{m}$  and 340  $\mu\text{m}$ . However, the elastic modulus increased with the paper thickness (Figure 3b). The elastic modulus of a carbon Miura-ori derived from the CG paper with an initial paper thickness of 190  $\mu\text{m}$  was  $111.08 \pm 59.65$  kPa, whereas CG paper thickness of 340  $\mu\text{m}$  resulted in an elastic modulus of  $307.42 \pm 66.01$  kPa for a similar geometry of the Miura-ori structure. Our hypothesis for such variation of elastic modulus with the paper thickness was that the occurrences of fiber entanglement increase along the thickness of the paper as the paper thickness increases. These fiber entanglements act as the resistance under a compressive load. Due to these enhanced resistances, the carbon Miura-ori structures with thicker paper exhibited higher mechanical stiffness. Furthermore, higher paper thickness yielded a higher structural density. Inset of Figure 3b shows that the geometric dimensions of the carbon Miura-ori structures

remained unchanged for both the paper thicknesses. However, total mass of the carbon Miura-ori increased with higher paper thickness, which further resulted in higher structural density. It is mentioned earlier that the elastic modulus of an architected structure is proportional to its structural density. Therefore, the higher structural density resulted in from the paper thickness also contributed to the enhanced elastic modulus of the origami shapes with thicker cross-section.

### 3.4 Using processing variables to effect the density and elastic modulus of Carbon Origami

We plotted the elastic moduli of the all the carbon Miura-ori structures obtained at different conditions against their structural densities in Figure 4a to compare the effect of different processing variables. To emphasize the effect of the variables, we also plotted linear tradelines for each variable in Figure 4b. Here, a stiffer slope indicates a more influential variable, which can result in a higher elastic modulus with a minimum alteration of the density. Among all the parameters, combination of the design angle  $\alpha$  and the folding angle  $\beta$  seemed to be the most influencing parameter for determining the elastic modulus of the carbon Miura-ori shapes. For example, changing  $\beta$  with the  $\alpha$  of  $41^\circ$  resulted in a slope of  $8117.3 \text{ m}^2/\text{s}^2$ , whereas the slope for the  $\alpha$  of  $75^\circ$  was  $27485.0 \text{ m}^2/\text{s}^2$ . The slopes for other variables were within these two values. This suggests that the elastic modulus of the carbon Miura-ori structures can be modulated within a wide range just by tuning the geometric features  $\alpha$  and  $\beta$ . This further suggests that optimization of  $\alpha$  and  $\beta$  can yield to a carbon Miura-ori with the highest possible elastic modulus. Our ongoing work includes a numerical simulation towards optimization of these two variables to determine the highest elastic modulus.

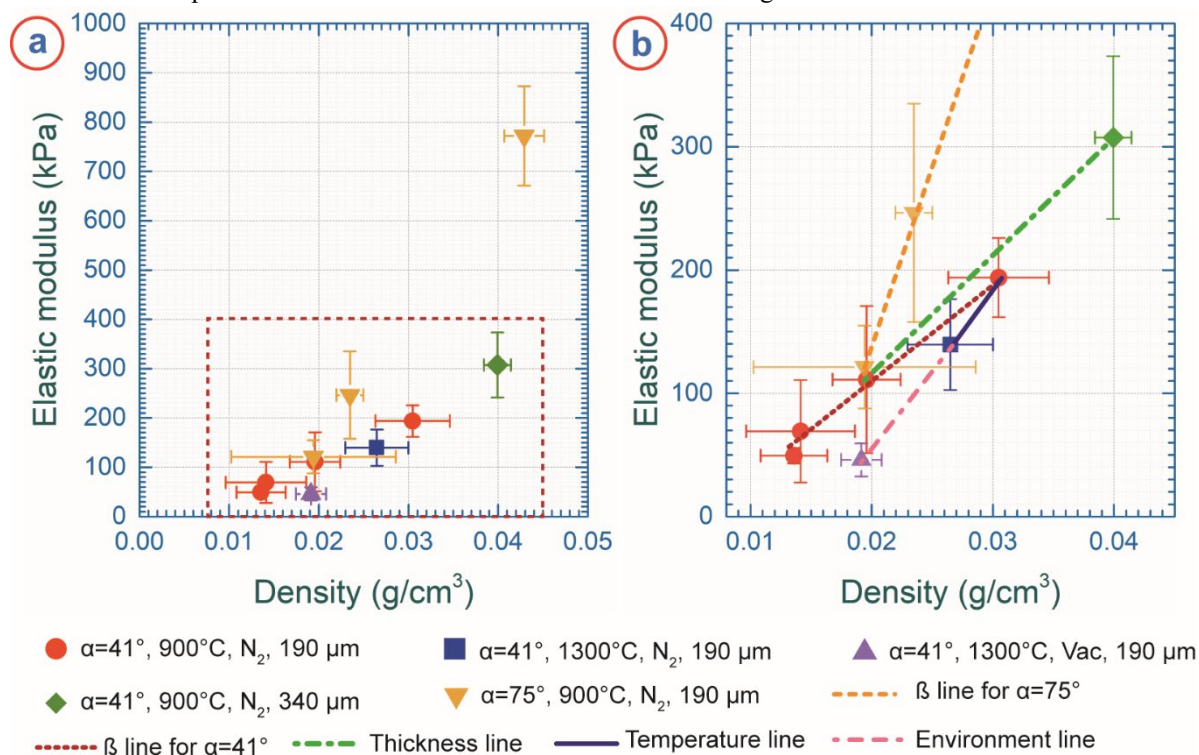


Figure 4: (a) Elastic modulus vs density of all the carbon Miura-ori structures fabricated using different combinations of the processing variables. The data points within the red dashed rectangle in (a) are plotted in (b) for clarity. Linear tradelines are also plotted in (b) for each processing parameter to compare the effect of the processing variables.

#### 4. Conclusion

Here we reported a study on the effect of different process parameters on the mechanical properties of carbon origami structures. A vacuum environment versus a nitrogen environment had a stronger impact on the density and mechanical properties of the carbon origami structure, compared to the effect of final temperature of the carbonization process. A vacuum environment resulted in a significantly lighter carbon origami structure, due to generation of highly porous carbon microstructure. Such carbon origami structures obtained in vacuum environment exhibited lower elastic modulus. Furthermore, the elastic modulus exhibited a proportional relation to the design angle  $\alpha$  and an inversely proportional relation to the folding angle  $\beta$ . Although the paper thickness did not have any noticeable effect on the geometry of the carbon Miura-ori structure, a higher elastic modulus was achieved for a higher paper thickness. The combination of the geometrical features  $\alpha$  and  $\beta$  was found to be the most influential variable among all the variables studied here. Combination of  $\alpha$  and  $\beta$  can result in elastic modulus within a wide range. An optimization of these two variables is needed to find the combination for the highest possible elastic modulus of carbon Miura-ori.

Although the current results show the dependence of mechanical behavior of the carbon origami shapes on its microstructure and geometrical features, further investigation is needed to fully elucidate the relation among the microstructure, geometry, and macrostructural properties of the carbon origami shape. Such investigation can lead us to design carbon origami shapes with mechanical properties close to the theoretical limits at a low density.

#### Acknowledgements

Monsur Islam acknowledges support from Hitachi through Hitachi High Technologies Electron Microscopy Fellowship. The authors are thankful to the Institute for Biological Interfaces of Engineering for facilitating the mechanical testing and to Prof. Suyi Li at Clemson University for discussion regarding the structure of Miura-ori.

#### Authors' contribution

Conceptualization, M.I. and R.M.-D.; Data curation, M.I.; Formal analysis, M.I. and R.M.-D.; Investigation, M.I.; Methodology, M.I. and R.M.-D.; Project administration, R.M.-D.; Supervision, R.M.-D.; Validation, M.I.; Writing—original draft, M.I.; Writing—review & editing, M.I. and R.M.-D.

#### References

- [1] M. Inagaki, J. Qiu, Q. Guo, Carbon foam: Preparation and application, *Carbon N. Y.* 87 (2015) 128–152. doi:10.1016/j.carbon.2015.02.021.
- [2] K.Y. Foo, B.H. Hameed, Mesoporous activated carbon from wood sawdust by  $K_2CO_3$  activation using microwave heating, *Bioresour. Technol.* 111 (2012) 425–432. doi:10.1016/j.biortech.2012.01.141.
- [3] G.M. Duran, T.E. Benavidez, J.G. Giuliani, A. Rios, C.D. Garcia, Synthesis of CuNP-modified carbon electrodes obtained by pyrolysis of paper, *Sensors Actuators B Chem.* 227 (2016) 626–633. doi:10.1016/j.snb.2015.12.093.
- [4] M. Islam, P.G. Weidler, S. Heissler, D. Mager, J.G. Korvink, Facile template-free synthesis of multifunctional 3D cellular carbon from edible rice paper, *RSC Adv.* 10 (2020) 16616–16628. doi:10.1039/D0RA01447H.
- [5] Z.-Y. Wu, C. Li, H.-W. Liang, J.-F. Chen, S.-H. Yu, Ultralight, Flexible, and Fire-Resistant Carbon Nanofiber Aerogels from Bacterial Cellulose, *Angew. Chemie Int. Ed.* 52 (2013) 2925–2929. doi:10.1002/anie.201209676.
- [6] M. Islam, R. Martinez-Duarte, The impact of using different renewable films in the synthesis and microstructure of carbonaceous materials applicable in origami-inspired manufacturing, *Materialia.* 11 (2020) 100734. doi:10.1016/j.mtla.2020.100734.
- [7] M. Islam, J. Flach, R. Martinez-Duarte, Carbon origami: A method to fabricate lightweight carbon cellular materials, *Carbon N. Y.* 133 (2018) 140–149. doi:10.1016/j.carbon.2018.03.033.
- [8] B. Cowan, P.R. von Lockette, Fabrication, characterization, and heuristic trade space exploration of magnetically actuated Miura-Ori origami structures, *Smart Mater. Struct.* 26 (2017) 045015. doi:10.1088/1361-665X/aa5a9e.
- [9] Q. Cheng, Z. Song, T. Ma, B.B. Smith, R. Tang, H. Yu, H. Jiang, C.K. Chan, Folding Paper-Based Lithium-Ion Batteries for Higher Areal Energy Densities, *Nano Lett.* 13 (2013) 4969–4974. doi:10.1021/nl4030374.

- [10] M. Islam, Advanced Manufacturing of Lightweight Porous Carbide Shapes Using Renewable Resources, 2018.  
[https://tigerprints.clemson.edu/all\\_dissertations](https://tigerprints.clemson.edu/all_dissertations).
- [11] S.M. Manocha, K. Patel, L.M. Manocha, Development of carbon foam from phenolic resin via template route, *Indian J. Eng. Mater. Sci.* 17 (2010) 338–342.
- [12] M. Islam, D. Keck, R. Martinez-Duarte, Architected Tungsten Carbide Electrodes Using Origami Techniques, *Adv. Eng. Mater.* 21 (2019) 1900290. doi:10.1002/adem.201900290.
- [13] M. Islam, A.D. Lantada, M.R. Gómez, D. Mager, J.G. Korvink, Microarchitected Carbon Structures as Innovative Tissue Engineering Scaffolds, *Adv. Eng. Mater.* (2020) adem.202000083. doi:10.1002/adem.202000083.
- [14] M.F. Ashby, *Materials Selection in Mechanical Design*, Fourth edi, Elsevier Ltd., 2011.
- [15] B. Dickens, Thermally degrading polyethylene studied by means of factor-jump thermogravimetry, *J. Polym. Sci. Polym. Chem. Ed.* 20 (1982) 1065–1087.